Extracting the dynamics in classically chaotic quantum systems: Spectral analysis of the HO_2 molecule

Jörg Main
Institut für Theoretische Physik I, Ruhr-Universität Bochum, D-44780 Bochum, Germany

Christof Jung
UNAM Instituto de Matematicas, Unidad Cuernavaca, Av. Universidad s/n, 62251, Cuernavaca, Mexico

Howard S. Taylor
Department of Chemistry, University of Southern California, Los Angeles, California 90089

(Received 19 May 1997; accepted 30 July 1997)

We present a scaling technique to analyze quantum spectra, i.e., to obtain from quantum calculations detailed information about the underlying important classical motions. The method can be applied to a general quantum system without a classical scaling property. A demonstration on the conventionally unassignable vibrational spectrum of the HO_2 radical reveals remnants of classical broken tori embedded in the chaotic phase space and leads to a new assignment of spectral patterns in terms of classical Fermi resonances between the local mode motions. The scaling technique also allows to investigate the statistical properties of level spacings at fixed energies. The nearest neighbor spacing distribution of the HO_2 molecule undergoes a transition from mixed phase space behavior at low energies to the Wigner distribution characteristic for chaotic systems at energies near the dissociation threshold. © *1997 American Institute of Physics.* [S0021-9606(97)03741-0]

I. INTRODUCTION

Quantum spectra of classically regular systems are interpreted in terms of the underlying classical dynamics that influence the quantum spectra, e.g., in molecules often the normal or local mode vibrational motions that take place on stable tori in phase space.[1] Since many systems, especially upon excitation show classically chaotic motion, it is of fundamental importance to perform an analogous analysis for chaotic systems, i.e., to extract information about the important classical motions directly from quantum spectra and to assign spectral patterns in terms of broken tori or unstable periodic orbits.[2] This is a nontrivial problem especially if the underlying classical dynamics of the quantum system changes significantly with energy. Exceptions are systems possessing a classical scaling property, i.e., the same classical phase space structure for all values of an appropriate scaling parameter. The scaling parameter is usually some power of an external field strength or, for Hamiltonians with homogeneous potentials, the energy. Such scales can be controlled in the laboratory and spectra can be taken as a function of the scaling parameter. Examples are the three-body Coulomb system[3] or atoms in magnetic fields[4] where information about the underlying classical dynamics can be extracted from quantum spectra by application of *scaled-energy spectroscopy*.[5,6] In contrast, e.g., molecular vibrational Hamiltonians are prototypical examples of classically nonscaling systems.

Here we present an extended version of the scaling technique which does not allow scaled-energy spectroscopy in the lab but can be applied in theoretical quantum calculations to provide information on the classical dynamics, periodic motions, and statistical properties of spectra at any given energy. Such information cannot be obtained from a single eigenstate ψ_n at energy $E=E_n$ but only from many states at energies around E. Analyzing these states automatically implies a smoothing over the energy. The aim of the scaling technique is to obtain additional information by creating a family of quantum systems all of which have the same underlying classical dynamics at energy E. The eigenstates of these systems can be analyzed without any smoothing in energy to create a diagram which highlights at any given energy, certain values of the periods. Classical trajectory calculations, by finding periodic orbits with matching periods, then reveal those motions and phase space structures that influence both the regular and irregular quantum spectra. The importance of the method is for chaotic dynamics as regular systems are well understood.[1,7]

II. THE CONCEPT OF THE SCALING TECHNIQUE

Consider a multidimensional system given by the Hamiltonian $H=T+V(\mathbf{q})$ with a general nonhomogeneous potential $V(\mathbf{q})$. For simplicity we assume $T=\mathbf{p}^2/2m$ in the following. Generalizations of the scaling technique to more complex representations of the kinetic energy will be straightforward. The basic idea is to enlarge formally the parameter space of the potential $V(\mathbf{q})$ by introducing an additional parameter z. The dependence of the potential on z is defined by

$$V(\mathbf{q};z)=V(\mathbf{q}/z;z=1)=V(\mathbf{q}/z)=V(\tilde{\mathbf{q}}), \tag{1}$$

where $\tilde{\mathbf{q}}=\mathbf{q}/z$ are scaled coordinates, i.e., z is a scaling parameter describing a blow up or shrinking of the potential, with $z=1$ corresponding to the true physical situation. It follows that $V(\mathbf{q};z)$ is the value of the original potential at $\mathbf{q}/z$. By considering the family of systems given by the Lagrangian

$$L = m\dot{\mathbf{q}}^2/2 - V(\mathbf{q};z) = mz^2\dot{\tilde{\mathbf{q}}}^2/2 - V(\tilde{\mathbf{q}}) \tag{2}$$

it is easy to show that $\tilde{\mathbf{p}} = z\mathbf{p}$ is the canonical conjugate momentum to $\tilde{\mathbf{q}}$. We can now consider the parametric family of Hamiltonians

$$H = \frac{1}{2m}\mathbf{p}^2 + V(\mathbf{q}/z) = \frac{1}{z^2}\frac{\tilde{\mathbf{p}}^2}{2m} + V(\tilde{\mathbf{q}}) = \frac{1}{z^2}T + V(\tilde{\mathbf{q}}). \tag{3}$$

The fact that the transformations of $\mathbf{p}$ and $\mathbf{q}$ are linear and canonical means that the Schrödinger quantization rules can be applied directly to the new variables $\tilde{\mathbf{q}}$ and $\tilde{\mathbf{q}}$. This also means that the classical motion and particularly the shape of classical (periodic) orbits are not affected by a consistent scaling. Orbits just blow up and shrink in the same way as the potential.

Considering now the quantum mechanics, obviously the systems have different quantum spectra for various z values. Each quantum Hamiltonian $H(z) = \tilde{\mathbf{p}}^2/2mz^2 + V(\tilde{\mathbf{q}})$ has an effective $\hbar$, $\hbar_{\text{eff}} = \hbar/z$ (or alternatively an effective mass $m_{\text{eff}} = mz^2$), i.e., the Hamiltonians $H(z)$ describe a family of quantum systems with the same underlying classical dynamics. The semiclassical and classical limits are reached as $z \to \infty$ ($\hbar_{\text{eff}} \to 0$). Note that so far the scaling parameter z is not a dynamical variable.

III. SCALED (E,z) DIAGRAM OF THE HO_2 MOLECULE

As an example to illustrate our scaling technique on a real system we study the vibrational spectrum of the hydroperoxyl radical, HO_2, which shows a classically chaotic dynamics. Using the potential surface of Pastrana *et al.*[8] 361 bound states have been calculated recently at the physical value $z = 1$.[9,10] Only about the 32 lowest states out of 361 bound states can be assigned[11] in the conventional regular spectra sense,[1] i.e., methods of fitting regular spectra fail at higher energies and wave functions show no regular patterns.[9] For the quantum calculation of eigenstates at various z values we use a DVR grid representation of basis functions and the computational method of filter diagonalization.[10] In a first step we diagonalize the Hamiltonian at a fixed value $z = 2$ with matrix dimension $> 100\,000$ and obtain about 2600 energy eigenvalues and eigenvectors of bound states. In a second step we use the eigenfunctions at $z = 2$ as a contracted basis set to calculate eigenvalues at arbitrary z values. Note that the first step, i.e., the diagonalization of the Hamiltonian at a fixed value z consumes most of the numerical resources like CPU time and storage. The second step, i.e., the calculation of spectra at various scaling parameters z requires the diagonalization of matrices of moderate dimensionality only and can be performed efficiently with standard diagonalization routines. Note also that the matrix representations of the kinetic energy T and the potential energy V in Eq. 3 do not depend on E and z and therefore need to be calculated only once.

A part of the (E,z)-diagram obtained for the HO_2 molecule is presented in Fig. 1a. For graphical purpose we plot in Fig. 1b $(E - E_b)z$ versus z where $E_b = -2.38$ eV is the bottom energy of the HO_2 potential surface. In the latter

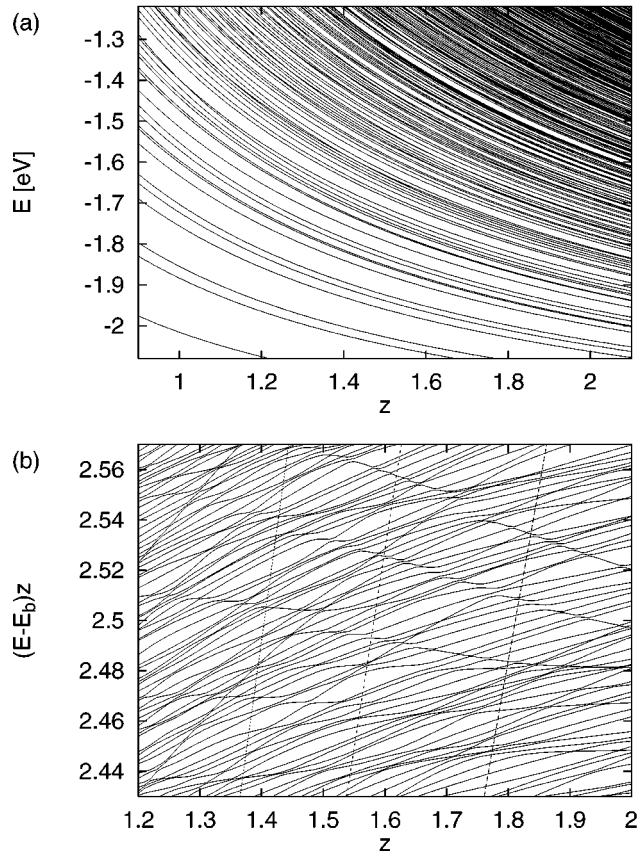

FIG. 1. Scaled spectra for the HO_2 molecule. (a) Energy E versus scale parameter z. (b) $(E - E_b)z$ versus z. The dashed lines mark lines of constant energy at (from the left) $E = -0.6$ eV, $E = -0.8$ eV, and $E = -1.0$ eV.

presentation the avoided crossings between levels become more pronounced and indicate the chaotic dynamics of the molecule.

IV. VIBROGRAM ANALYSIS OF SPECTRA

For completeness and to illustrate the differences to our new scaling method we describe here the conventional method of analyzing the quantum spectra at a fixed z parameter, e.g., for the physical system at $z = 1$. The classical dynamics and, in particular, the recurrence times of periodic orbits depend on the energy E. Therefore the Fourier transform of spectra along large energy regions can in general not be interpreted in terms of classical orbits. However, the energy can be approximately fixed by using a windowed Fourier transform (Gabor transform) of quantum spectra resulting in vibrograms being a function of energy and time,[12]

$$G_\sigma(E,T) = \int_{-\infty}^{+\infty} \varrho(E') e^{-iE'T/\hbar - (E-E')^2/2\sigma^2} dE', \tag{4}$$

with σ being the width of the Gaussian energy window. This analysis has been applied to various classically nonscaling systems[13,14] and has the advantage that it can be directly applied to experimental spectra. The vibrogram for the HO_2 molecule at the physical scaling parameter $z = 1$ is shown in Fig. 2a. The diagram is not adequate to correlate its broad

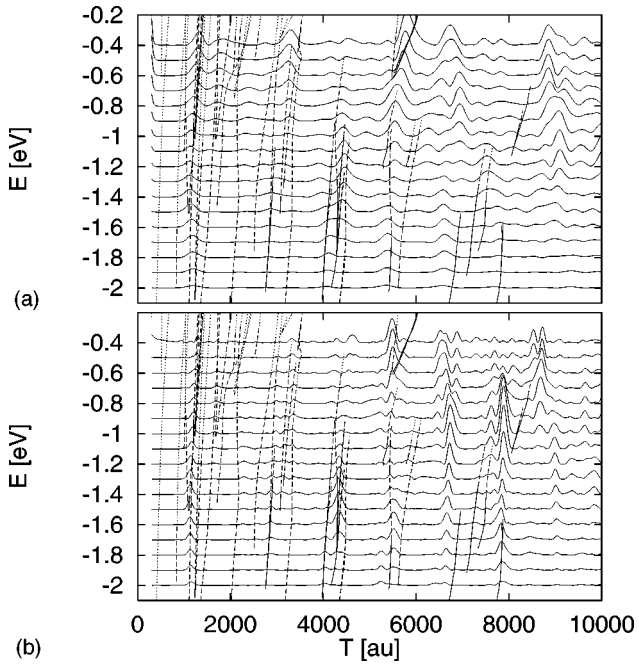

FIG. 2. Vibrogram analysis of the HO_2 spectra with energy smoothing width $\sigma=0.2$ eV. (a) $z=1$, (b) $z=2$. Dashed lines: Part of the classical bifurcation diagram.

peaks to specific longer periodic orbits. The resolution of vibrograms in energy and time is fundamentally restricted by Heisenberg's uncertainty principle[13]

$$\Delta E \cdot \Delta T \approx \hbar_{\text{eff}} = \hbar/z. \tag{5}$$

To improve the resolution and to relate quantum structures to various classical orbits, the effective $\hbar$ has to be reduced in theoretical calculations.[14] Figure 2b presents the vibrogram for the HO_2 molecule analyzed along the line $z=2$ in Fig. 1. The resolution is considerably improved. However, the experimental connection is eliminated for $z\neq 1$ and in this case, as in the scaling technique, the conventional vibrogram analysis needs the knowledge of the potential surface to calculate quantum spectra. For interpretation in terms of classical orbits and comparison to the classical bifurcation diagram a potential is needed for either method.

In the following we introduce our scaling technique. The method works at single energies and the resolution is not restricted by the uncertainty principle.

V. SEMICLASSICAL ANALYSIS OF THE SCALED SPECTRA

The decisive step for the scaling technique is to analyze the eigenvalues (eigenvectors are not needed) in Fig. 1 not along a line of constant z but along lines of constant energy E (dashed lines in Fig. 1b). From the eigenvalues $z_i(E)=z_i^E$ at constant energy E we obtain the density of states $\varrho^E(z)=\Sigma_i \delta(z-z_i^E)$ as a function of z. This is equivalent to considering the scaling parameter z as a new dynamical variable and rewriting Schrödinger's equation

$$\left[\frac{1}{z^2}T+V(\tilde{\mathbf{q}})\right]|\psi\rangle = E|\psi\rangle \tag{6}$$

for a particular fixed value of the energy E as a Hermitian eigenvalue equation for $\lambda=z^{-2}$,

$$T^{-1/2}[E-V(\tilde{\mathbf{q}})]T^{-1/2}|\Phi\rangle = \frac{1}{z^2}|\Phi\rangle; \quad |\Phi\rangle = T^{1/2}|\Psi\rangle, \tag{7}$$

where $T=\tilde{\mathbf{p}}^2/2m$ is the operator of scaled kinetic energy. Clearly, the eigenvalue equation (7), when diagonalized at various energies E, also gives Fig. 1. The new Hamiltonian on the left can be used to formally set up the Green's function and density of states

$$G^E(\lambda)=[\lambda - T^{-1/2}(E-V)T^{-1/2}]^{-1}, \tag{8}$$

$$\varrho^E(z)=\frac{2}{\pi z^3}\,\text{Im Tr}G^E(\lambda) = -\frac{2}{z^3}\sum_i \delta(\lambda-\lambda_i^E) = \sum_i \delta(z-z_i^E). \tag{9}$$

For the interpretation of the quantum mechanically calculated $\varrho^E(z)$ we can now involve the semiclassical theories, in particular, the Berry-Tabor formula for semiclassical torus quantization[15] or here Gutzwiller's periodic orbit theory for the semiclassical density of states of classically chaotic systems.[2] Gutzwiller's trace formula gives the semiclassical approximation to Eq. 9 as

$$\varrho^E(z)=\varrho_0^E(z)+\sum_{\text{p.o. }k} A_k \sin\left(z\tilde{S}_k-\frac{\pi}{2}\mu_k\right), \tag{10}$$

where $\varrho_0^E(z)$ is the mean level density, A_k is the amplitude related to the stability matrix of periodic orbit k, μ_k the Maslov index, and $\tilde{S}=S/z$ the scaled classical action which can also be proven to be the canonically conjugate variable to z. Information about the classical dynamics can now be obtained *from the quantum recurrence spectra* by a Fourier transform of $\varrho^E(z)$. From Eq. 10 it follows that each peak in the Fourier transformed action spectra can be identified either with an individual periodic orbit or with a braid of orbits with similar shapes and periods related to a broken resonance torus.

For the HO_2 molecule the Fourier transform action spectra along lines of constant energy are presented in Fig. 3 in overlay form in the region -2.0 eV$<E<-0.2$ eV. We also performed an extensive periodic orbit search. The quantum recurrence spectra are superimposed on the classical bifurcation diagram (dashed lines in Fig. 3) obtained from the classical calculations. The total number of periodic orbits in this three-dimensional system is incredibly high even in the limited range of actions $\tilde{S}/2\pi<80$ selected in Fig. 3. For the comparison with the quantum spectra we are not interested in orbits which change their stability properties (e.g., the Liapunov exponents) rapidly with the energy. In Fig. 3 we included only orbits which are not extremely unstable and where the Liapunov exponents are smooth functions of the energy within longer energy intervals. Details of the classical

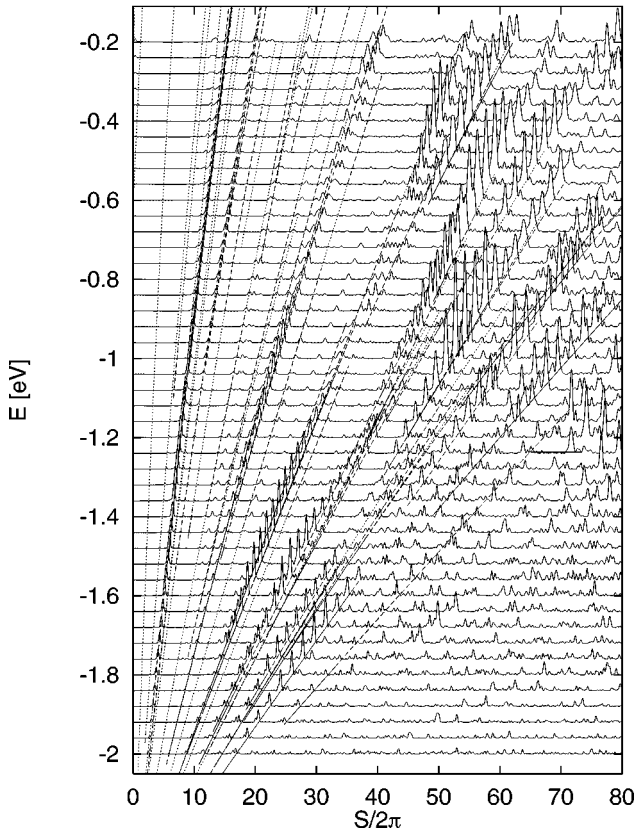

FIG. 3. Magnitude square of the Fourier transformed scaled spectra $\varrho^E(z)$ of the HO_2 molecule. The action spectra are superimposed on the classical bifurcation diagram (dashed lines).

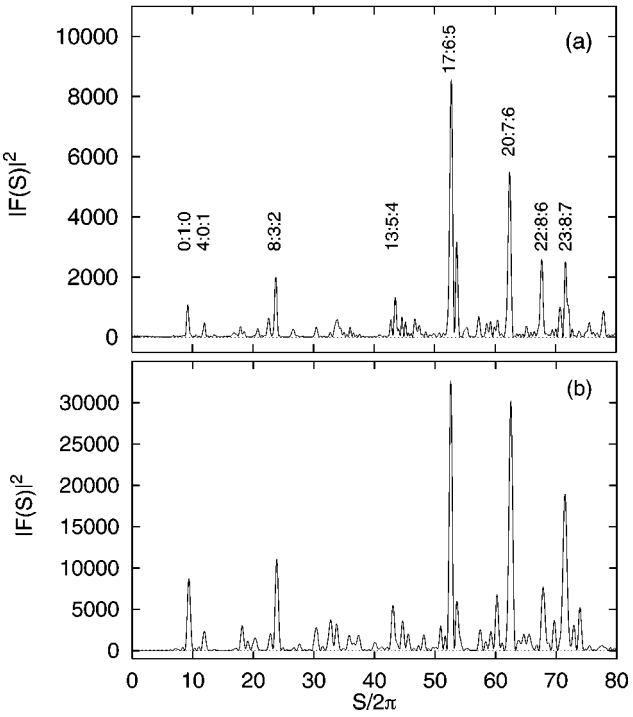

FIG. 4. (a) Fourier transform density of states at constant energy $E=-1.0$ eV. Some peaks are assigned by frequency ratios of classical trajectories on broken resonance tori. (b) Fourier transform of semiclassically calculated density of states.

calculations will be given elsewhere. The quantum spectra show very sharp and detailed structures. The sharpness of peaks in the Fourier transform indicates the importance of a particular orbit or braid of orbits along the whole range of z values (classical to quantum). The quantum mechanically obtained peak heights are related to the amplitudes A_k of periodic orbits in Gutzwiller's trace formula (Eq. 10). A direct semiclassical calculation of these peaks for a chaotic 3D system is a presently unachievable task requiring, to determine which orbits are important, the finding of *all* periodic orbits up to a certain period. Indeed, a careful examination of Fig. 3 shows that not all quantum structures are explained by those orbits that we have numerically found. On the other hand orbits not highlighted in Fig. 3, which are needed to converge the periodic orbit sum (Eq. 10), do not make major qualitative contributions to the quantum dynamics. The highlighted periodic orbit structures (which might be isolated orbits or broken resonance tori if families of similar periodic orbits exist under one peak) are the classical motions which determine the quantum spectra up to intermediate resolution. These structures are markers for regions in phase space where the dynamical potential causes trapping seen by quantum mechanics.[16]

The periods and amplitudes of the important structures highlighted in Fig. 3 depend on the energy. For example there is a weak resonance structure around $E=-1.2$ eV, $\tilde{S}/2\pi=45$ whose intensity increases at higher energies to maximum strength around $E=-1.0$ eV, $\tilde{S}/2\pi=52$ and then decreases again. Here highlighted periodic orbits show that such structures can be explained by classical trajectories moving on broken resonance tori. The individual peaks being associated with recurrent motion have rational frequency ratios $\nu_1:\nu_2:\nu_3$ between the three local mode motions, viz. the O-H stretch, the O-O-H bending, and the O-O stretch. Interestingly most of the stronger peaks in Fig. 3 can be identified and assigned in this way, i.e., they represent classical Fermi resonances between the local modes. Figure 4a shows as an example the assignments of the important structures in the scaled action spectrum at constant energy $E=-1.0$ eV. (If one or two local mode motions have nearly zero amplitude we assign these modes formally by frequencies $\nu=0$.) The two strongest peaks at $\tilde{S}/2\pi=52.5$ and $\tilde{S}/2\pi=61.9$ belong to frequency ratios $\nu_1:\nu_2:\nu_3=17:6:5$ and 20:7:6. These peaks can be related to families of similar periodic orbits localized in phase space, two members are shown in Fig. 5 in projections of the local mode coordinates.

In Fig. 6 we present for some trajectories the Fourier transform of the local mode motions, i.e., the O-O-H bending (full line), the O-O stretch motion (dashed line), and the O-H stretch motion (dotted line). Such figures can serve to identify the type of motion for periodic orbits or segments of trajectories on broken tori. For example, Figs. 6a and 6b show dominant O-O-H bending and O-O stretch motion, respectively and these types of motion are related to the first two peaks in the action spectra (see Fig. 4). In Figs. 6c and 6d all three local modes are excited with the frequency ratios

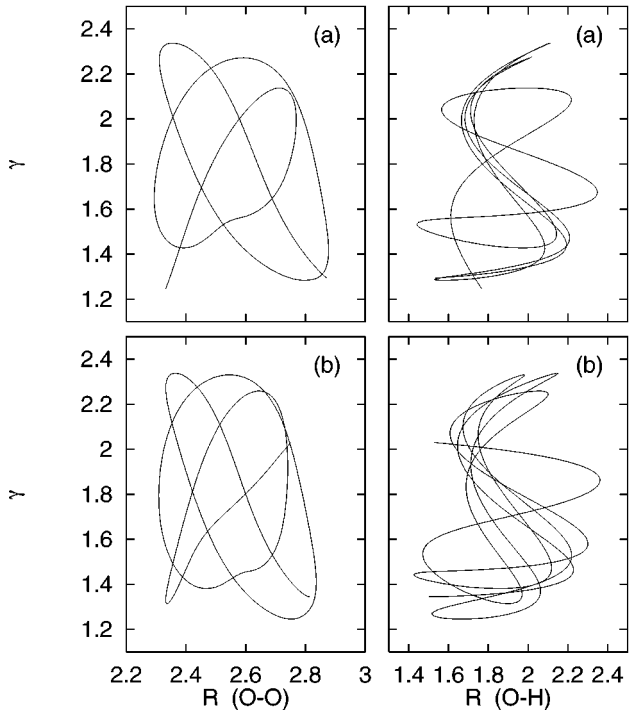

FIG. 5. Projections of a periodic orbit at energy $E=-1.0$ eV in local mode coordinates R_{OO}, R_{OH}, and bending angle γ. (a) Periodic orbit with classical action $\widetilde{S}/2\pi=52.5$ and frequency ratio 17:6:5. (b) $\widetilde{S}/2\pi=61.91$, frequency ratio 20:7:6.

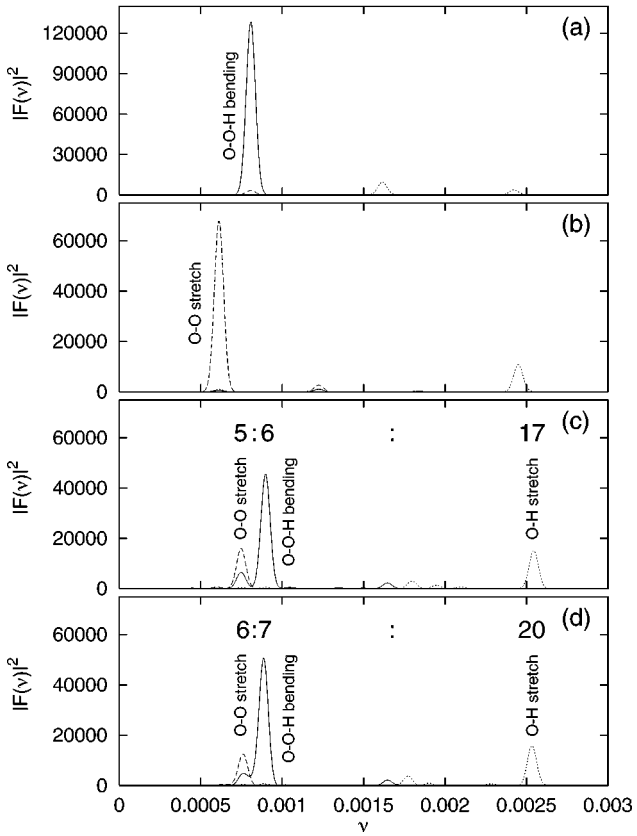

FIG. 6. Fourier transforms of local mode motions of classical trajectories. Energy $E=-1.0$ eV.

$\nu_1:\nu_2:\nu_3=17:6:5$ and 20:7:6 of the orbits presented in Fig. 5 and can identify the correspondingly marked peaks in Fig. 4. In fact, in place of the labor intensive periodic orbit search used to identify the dynamics under the peaks, the periodic orbits highlighted by the scaling technique seem to be sufficiently robust that time segments of a long trajectory can be Fourier analyzed to see if the frequencies of the three local mode motions are in rational ratio.[17] If they are the trajectory segment lies close to important periodic orbits and can be used to find these highlighted orbits rather easily.

VI. SEMICLASSICAL CALCULATION OF SCALED RECURRENCE SPECTRA

In the previous section we applied Gutzwiller's periodic orbit formula (10) for the interpretation of quantum recurrence spectra in terms of classical periodic orbits. At this point it might be asked why not simply sum the periodic orbit contributions in Gutzwiller's trace formula (10) in the first place? The answer is that the periodic orbit search for systems with three or more degrees of freedom is much more work and introduces significantly more numerical ambiguities than the scaled quantum calculation as a function of z. To do the periodic orbit summation essentially all orbits at given energy, including those near bifurcations, have to be found and their semiclassical amplitudes calculated. Our method is to first find the important periods (the highlighted peaks in Fig. 3) by quantum calculations and then to use, e.g., the segmented trajectory method to find the robust motions under the most important peaks.

At energy $E=-1.0$ eV we have taken on the task of the direct summation of periodic orbit contributions using a limited set of orbits to construct the semiclassical recurrence spectrum in the region $\widetilde{S}/2\pi<80$. In our opinion it is impossible right now to find the complete set of periodic orbits up to this action for the three-dimensional HO_2 molecule and we restricted our periodic orbit search to those orbits which have a turning point on the potential surface $V=E$. This constraint reduces the dimension of space for the initial conditions from four to two. The extensive search yielded more than 800 periodic orbits with classical action $\widetilde{S}/2\pi<80$ which are nearly densely distributed along the whole range of action. However, most of the orbits are extremely unstable, i.e., their Liapunov exponents are very high. Inserting the periodic orbit parameters into Gutzwiller's trace formula (10) for the scaled system at fixed energy and calculating the Fourier transform we obtain the semiclassical recurrence spectrum presented in Fig. 4b. We excluded some orbits in the periodic orbit sum (10) which are very close to bifurcations and result in unphysically high recurrence peaks. In principle, for these orbits uniform semiclassical approximations[18] must be considered, but this remains to be done in future work. Interestingly and perhaps luckily the semiclassical recurrence spectrum (Fig. 4b) reproduces the main features observed in the quantum recurrence spectrum in Fig. 4a.

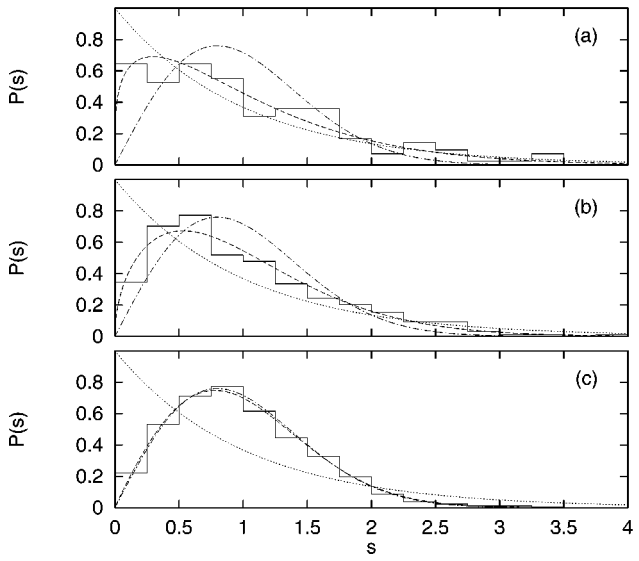

FIG. 7. Nearest-neighbor-spacing distribution of eigenvalues at constant energies (a) $E=-1.80$ eV, (b) $E=-1.40$ eV, and (c) $E=-0.20$ eV. Dotted lines: Poisson distribution; dashed-dotted lines: Wigner distribution; dashed lines: Brody distribution with (a) $q=0.25$, (b) $q=0.50$, and (c) $q=0.95$.

VII. STATISTICAL ANALYSIS OF NEAREST NEIGHBOR SPACINGS

It is well established that the nearest neighbor spacing distribution of integrable quantum systems after unfolding of the spectra to unit mean level spacing $\langle s\rangle=1$ is given by a Poisson distribution

$$P_{\text{Poisson}}(s)=e^{-s}, \tag{11}$$

while quantum systems with a fully chaotic (ergodic) underlying classical dynamics are characterized by the Wigner distribution

$$P_{\text{Wigner}}(s)=\frac{\pi s}{2}e^{-\pi s^2/4} \tag{12}$$

obtained from random matrix theory.[19] In systems with a mixed regular-chaotic classical dynamics the nearest neighbor spacing distribution can be phenomenologically described by the Brody distribution[20]

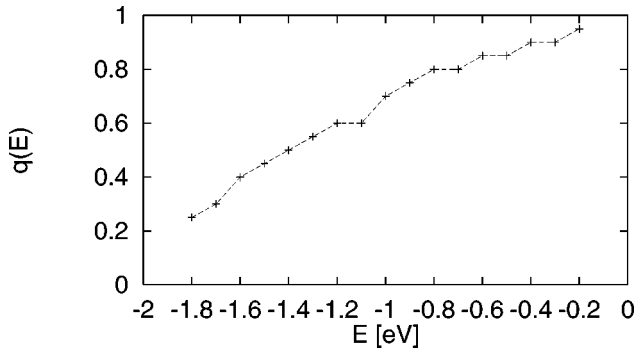

FIG. 8. Brody parameter q as a function of the energy for the scaled nearest-neighbor-spacing distributions of the HO_2 molecule.

$$P_{\text{Brody}}(s;q)=(q+1)\beta s^q e^{-\beta s^{q+1}}, \tag{13}$$

where

$$\beta=\left[\Gamma\left(\frac{q+2}{q+1}\right)\right]^{q+1}, \tag{14}$$

and q is a parameter which interpolates between the Poisson distribution ($q=0$) and the Wigner distribution ($q=1$) and is roughly related to the percentage of chaotic phase space volume of the underlying classical system.

For the HO_2 molecule the nearest neighbor spacing distribution of the 361 bound states has been calculated. The fit to the Brody distribution gives $q=0.92$.[9] This analysis, however, does not give any information about statistical properties in various energy regions. The problem is that short range energy intervals do not contain a sufficient number of states to carry out a statistical analysis. Here the scaling method can be applied to generate additional mono-energetic quantum information for such an analysis. More precisely, the additional quantum information in the scaled (E,z) diagram of Fig. 1a can be used to study the energy dependence of nearest neighbor spacing distributions by analyzing the (unfolded) level spacings $\Delta z_i^E=z_{i+1}^E-z_i^E$ along lines of constant energy E. Results are presented at three different energies in Fig. 7. At low energy $E=-1.80$ eV the spacing distribution can be fitted by a Brody distribution with $q=0.25$ which indicates a mixed regular-chaotic behavior of the underlying classical dynamics. The Brody parameter as a function of the energy, $q(E)$, is shown in Fig. 8. The Brody parameter grows with increasing energy and the nearest neighbor spacing distribution at $E=-0.20$ eV is close to the Wigner statistics characteristic for classically chaotic systems. The transition from almost regular to chaotic behavior can be explained by anharmonicities of the potential surface which increase with energy and cause a break down of more and more torus structures in the classical phase space. The deviations of $q(E)$ from a smooth curve in Fig. 8 are probably caused by numerical ambiguities.

VIII. CONCLUSION

The scaling technique introduced here is a powerful tool to analyze quantum spectra of systems not possessing a scaling property and to obtain information about the important classical dynamics, torus structures, and periodic orbits, that underly the quantum motion, directly from quantum calculations. The scaling technique also simplifies direct applications of semiclassical theories in that it allows to generate semiclassical spectra from periodic orbits calculated at a *single* energy and provides additional mono-energetic quantum information for a detailed statistical analysis of spectral properties. Application to the HO_2 molecule reveals remnants of broken tori in classical phase space related to Fermi resonances between the local mode motions and shows a transition from mixed regular-chaotic to completely chaotic dynamics in the nearest neighbor spacing distributions.

Finally we note in retrospect that no, even approximate, 2D tori were observed in the classical calculations indicating

that an approximate quantum number (polyad number) can not be defined for the very chaotic HO_2 radical. This prevents application of theories like that of Kellman[7] to this fully three-dimensional problem and the results of the present theory cannot be compared to such elegant methods.

ACKNOWLEDGMENTS

We acknowledge stimulating discussions with V. Mandelshtam, M. Kaluža, G. Ezra, and M. Davis and are grateful to V. Mandelshtam for supplying his program for filter diagonalization. This work was supported by DOE Grant number DE-FG03-94ER14458. J. M. is grateful to Alexander von Humboldt-Stiftung for a Feodor-Lynen scholarship, and to the college of Letters, Arts and Sciences for partial support of his visit at the University of Southern California. H. S. T. acknowledges the Alexander von Humboldt society for a Max Planck award which supported the visits during which this work was initiated.

[1] G. Herzberg, *Molecular Spectra and Molecular Structure* (Van Nostrand, Toronto, 1945, 1966), Vols. II and III.
[2] M. C. Gutzwiller, *Chaos in Classical and Quantum Mechanics* (Springer, New York, 1990).
[3] D. Wintgen, K. Richter, and G. Tanner, CHAOS **2**, 19 (1992).
[4] H. Friedrich and D. Wintgen, Phys. Rep. **183**, 37 (1989).
[5] A. Holle, J. Main, G. Wiebusch, H. Rottke, and K. H. Welge, Phys. Rev. Lett. **61**, 161 (1988).
[6] J. Main, G. Wiebusch, K. H. Welge, J. Shaw, and J. B. Delos, Phys. Rev. A **49**, 847 (1994).
[7] M. E. Kellman, in *Molecular Dynamics and Spectroscopy by Stimulated Emission Pumping*, edited by H.-L. Dai and R. W. Field (World Scientific, Singapore, 1995).
[8] M. R. Pastrana, L. A. M. Quintales, J. Brandao, and A. J. C. Varandas, J. Phys. Chem. **94**, 8073 (1990).
[9] A. J. Dobbyn, M. Stumpf, H.-M. Keller, and R. Schinke, J. Chem. Phys. **103**, 9947 (1995).
[10] V. A. Mandelshtam, T. P. Grozdanov, and H. S. Taylor, J. Chem. Phys. **103**, 10 074 (1995).
[11] D. H. Zhang and J. H. Zhang, J. Chem. Phys. **101**, 3671 (1994).
[12] B. R. Johnson and J. Kinsley, J. Chem. Phys. **91**, 7638 (1989).
[13] K. Hirai, E. J. Heller, and P. Gaspard, J. Chem. Phys. **103**, 5970 (1995).
[14] G. S. Ezra, J. Chem. Phys. **104**, 26 (1996).
[15] M. V. Berry and M. Tabor, Proc. R. Soc. London, Ser. A **349**, 101 (1976).
[16] G. Hose, H. S. Taylor, and Yi Yan Bai, J. Chem. Phys. **80**, 4363 (1984).
[17] G. S. Ezra, C. C. Martens, and L. E. Fried, J. Phys. Chem. **91**, 3721 (1987).
[18] J. Main and G. Wunner, Phys. Rev. A **55**, 1743 (1997).
[19] F. Haake, *Quantum Signatures of Chaos* (Springer, New York, 1991).
[20] T. A. Brody, J. Flores, J. B. French, P. A. Mello, A. Pandey, and S. S. M. Wong, Rev. Mod. Phys. **53**, 385 (1981).